M&C 2023 - The International Conference on Mathematics and Computational Methods Applied to Nuclear Science and Engineering · Niagara Falls, Ontario, Canada · August 13 – 17, 2023

Using Machine Learning to Unfold Neutron Spectra With a Passive Neutron Spectrometer

Z. Condon[1], D. Siefman[2], and R. Vasques[1]

[1]The Ohio State University, Department of Mechanical and Aerospace Engineering
201 W. 19th Avenue, Columbus, OH 43210, United States

[2]Lawrence Livermore National Laboratory
7000 East Avenue
Livermore, CA 94550

condon.87@buckeyemail.osu.edu, siefman1@llnl.gov, vasques.4@osu.edu

ABSTRACT

Unfolding neutron spectra is a heavily researched area due to the importance of neutron energy for determining radiation dose received. A novel detection system, the passive neutron spectrometer (PNS), is being investigated for use in energy spectrum unfolding techniques. The benefit of this detector is the passive detection of neutrons through the use of 55 thermoluminescent dosimeters or gold foils contained within a single polyethylene sphere. Multiple real-world detector responses were unfolded using the well-established MAXED algorithm as well as a novel neural network technique.

KEYWORDS: Passive Neutron Spectrometer, Spectrum Unfolding, Neural Networks

1. INTRODUCTION

The ability to unfold neutron spectra is a complex yet necessary challenge that is crucial for determining radiation dose. Accurately measuring and calculating this dose to within certain limits is a standard that is set by national and international government organizations [1]. On a regular basis, the capabilities of nuclear enterprises around the world are tested against these standards through international exercises [2]. Throughout these exercises, each organization acquires and compares dose information, which can have at most 20% error for gamma dose and 30% error for neutron dose measurements [1].

Acquiring accurate dose information from neutrons has been a difficult problem for many decades [3]. This difficulty stems from various factors. Unlike charged particles, neutrons do not experience any force in an electric field and high-voltage based detectors cannot force interactions. Additionally, the lack of charge results in a low linear energy transfer (LET) in many materials [4]. Similar to the reaction specific energy dependence of gamma rays, the likelihood of a neutron interacting in materials is heavily dependent on the neutrons' energy and the material through which the neutrons are travelling [5]. Some isotopes, such as Helium-3, have high probability of interaction with neutrons [6]. These types of reactions can release additional energy unique to the reaction in the form of gamma rays and other isotopes [4]. This adds additional difficulties in identifying the initial energy of the incident neutron.

To acquire dose information, an accurate representation of the neutron energies, or spectrum, is required. Neutrons of different energies cause different degrees of damage within the human body[7]. These energy dependencies are represented by dose equivalent coefficients, which are reported by the International Atomic Energy Agency (IAEA) in discrete energy bins ranging from 1E-9 MeV to 63 MeV[7]. Once the neutron spectrum is determined, the dose coefficients for each respective energy bin can be multiplied by the determined presence of each respective energy of neutron. Acquiring an accurate map of the neutron spectrum requires specialized detection methods as well as an algorithm to unfold the detector response.

The difficulty in unfolding the neutron spectrum lies in the fact that the energy of the neutron is connect be directly obtained from measurements. Current widely available neutron detectors consist of a material that has a high probability of interaction, known as the cross-section, with thermal neutrons [4]. These detectors require additional material, called a moderator, to slow down high-energy neutrons so that they can be detected [4]. Because interactions within this moderating material result in the loss of neutron spectrum information, various detector systems and algorithms have been developed to mitigate that information loss [3]. These systems and algorithms require input from subject matter experts for set up and execution.

The goal of this research is to determine if a novel detector, the passive neutron spectrometer (PNS) described in Section 2, can be used reliably for spectrum unfolding. This will be tested using the well-established MAXED algorithm and through a neural network trained using IAEA data, both described in Section 3. The choice to pursue a neural network approach was made because, once trained, the neural network would require only the detector response to calculate the associated energy spectrum. An additional benefit is that the calculation through the network is very fast compared to MAXED. In future work, the neural network approach will be further explored and optimized, but in this preliminary work, it will focus on proof-of-concept rather than optimization. This is due largely to the small data set obtained through the IAEA, which precludes a highly accurate network.

2. PASSIVE NEUTRON SPECTROMETER

To unfold neutron spectra, a variety of techniques are available, each with associated benefits and drawbacks. For example, Lithium-7 reacts with neutrons by converting to a Beryllium-7 atom and emitting a proton [8]. This proton has energy specific to the reaction, but is unrelated to the incident neutron energy [8]. Additionally, highly sensitive equipment can be used for time-of-flight measurements which directly measure the neutron spectrum by exploiting the difference in arrival times according to the energy of the neutron [9]. These types of measurements can only be conducted in a laboratory setting because they require near-instantaneous bursts of neutrons [9]. Another method employs multiple-sphere systems, called Bonner spheres, which consist of He-3 thermal neutron detectors surrounded by various size of moderating spheres [10]. Although moderating the neutrons causes a loss of information, varying sizes of the moderating spheres effects an energy dependence of the neutron flux at the detector. This energy dependence can be utilized following a series of detections by the whole system [10]. A drawback of this system is that multiple recordings need to occur, requiring the presence of an operator as well as a high-voltage power supply.

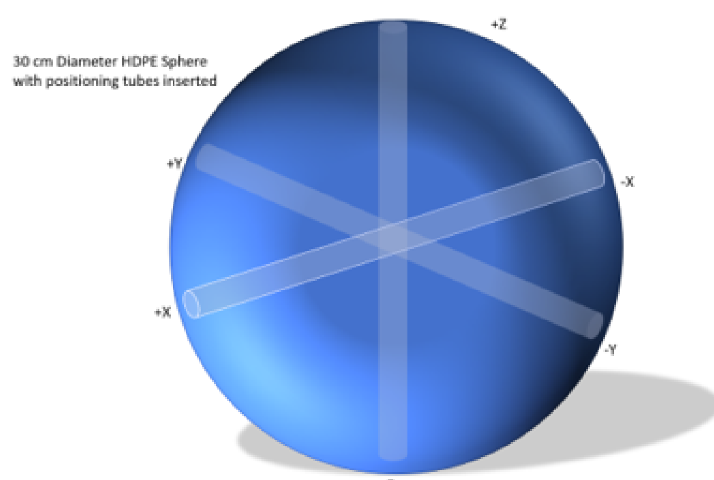

Figure 1: Model of the PNS

In previous work, the PNS was designed and shown to provide a new capacity for neutron spectrum unfolding [11]. It was then manufactured by Lawrence Livermore National Laboratory (LLNL) to explore this capacity. The design of the PNS incorporates 55 detectors, either thermoluminescent dosimeters (TLDs) or gold activation foils, placed within a 30-cm high-density polyethylene sphere. The detectors are placed at various locations along all three Cartesian axes. In all six directions ($\pm X$, $\pm Y$, $\pm Z$), the detectors are placed at the following distances from the center: 3 cm, 6 cm, 8 cm, 9 cm, 10 cm, 11 cm, 12 cm, 13 cm, and 14 cm. One final detector is placed at the center, orthogonal to the X-axis. A representation of the PNS is shown in Fig. 1. The major benefits of the PNS is that the detectors are all contained within one sphere, so only a single measurement in the neutron field is required. Additionally, because both TLDs and gold foils do not require power, the system will make all measurements passively.

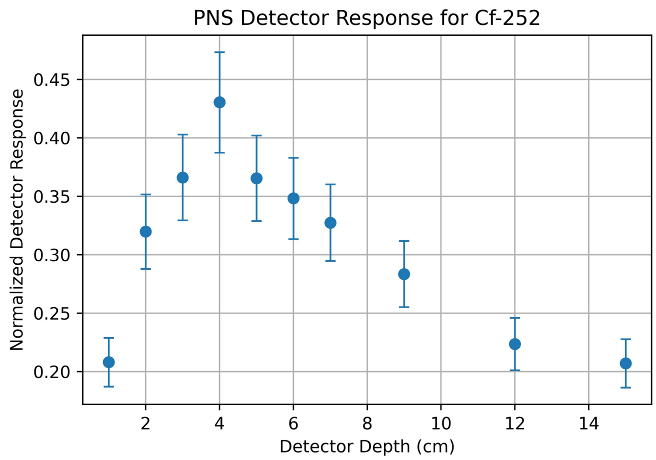

Figure 2: Depth-averaged detector response for the PNS

The collection of information recorded by the PNS is called the detector response (DR) and consists of 55 values, each corresponding to a detector. The spatial distribution of the detectors means that each detection depends on the position of the source and the location of the detector within the polyethylene sphere. For the early stages of this research, the detector response is simplified by averaging the responses that are at equal depths within the PNS, resulting in an array of 10 discrete values (see Fig. 2). This simplifies the initial investigation to determine the efficacy of the PNS at providing information to unfold the spectrum. After proof-of-concept, the entire DR can be used for establishing unfolding techniques and potentially developing directional detection capabilities. A similar detector, the Neutron Capture Therapy Wide Energy Spectrometer, has shown the ability to determine source direction [12].

The spectrum unfolding techniques outlined in this paper require the use of a detector response matrix (DRM), which contains the information for how each detector responds to monoenergetic neutrons. For the PNS, the DRM is of size 84×55, where 84 corresponds to the number of energy bins ranging from 1E-9 MeV to 20 MeV and 55 corresponds to each of the detectors. The number of energy bins was chosen to be 84 to be consistent with previous work relating to this detector.

Because monoenergetic neutron sources do not exist, the DRM was obtained through the Monte Carlo N-Particle (MCNP) code [13]. The full PNS was modeled with the TLDs placed as described earlier in this section and centered at the origin of the simulation. The TLDs modeled are made from Li-6 and Fluoride. The neutron source was modeled as a plane source orthogonal to the X-axis and placed at 25 cm from the center of the PNS. The neutron interactions were tallied using the +F6 tally within MCNP. See Fig. 3a for the full DRM. Similarly to the depth-averaged DR, the full DRM can also be depth-averaged to obtain a 84×10 matrix (see Fig. 3b).

3. NEUTRON SPECTRUM UNFOLDING

For a multi-detector system, like Bonner spheres or the PNS, the set of 55 detector responses and the corresponding neutron spectrum can be represented as a linear system of equations related by the DRM

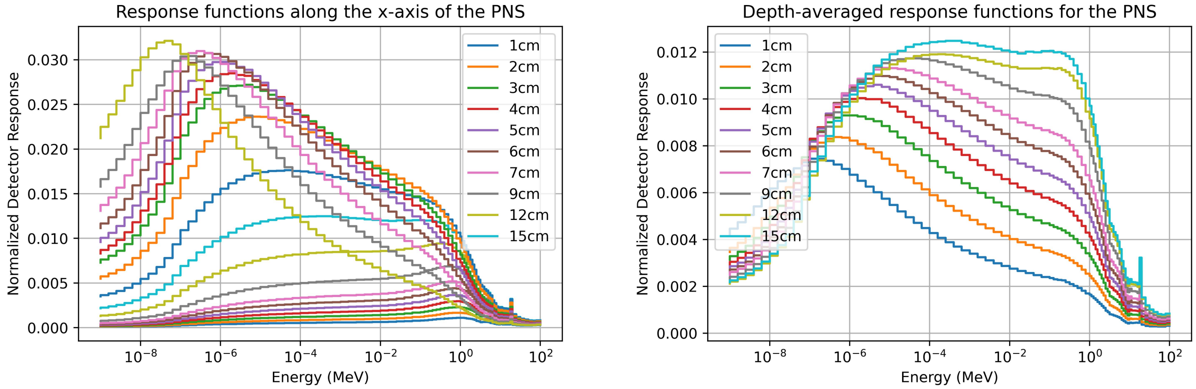

(a) X-axis detector response matrix **(b) Depth-averaged detector response matrix**

Figure 3: Detector response matrices for the X-axis and for the depth-averaged results for the PNS

[14]. This method requires the discretization of the continuous neutron energy spectrum into specific energy bins, as described above [14]. Then, by representing the discretized spectrum S as a $[1\times m]$ vector where m is the number of energy groups, and the measured detector response D as a $[1\times n]$ vector where n is the number of detector responses, the system can be written as Equation (1).

$$S_{[1\times m]}R_{[m\times n]} = D_{[1\times n]} \tag{1}$$

This equation introduces the final term, R, an $[m \times n]$ matrix which is the DRM. Mathematically, this equation can be solved for S, which would require pseudo-inverting the DRM. Unfortunately, the solution of the resulting linear equations is non-unique and cannot be used directly for spectrum unfolding.

3.1. MAXED Approach

A well-established approach for obtaining the unfolded neutron spectrum uses an iterative maximum-entropy method to acquire the true spectrum from the infinite space of all possible solution spectra [14]. This process has been named MAXED, which stands for Maximum Entropy Deconvolution [14]. To calculate the solution, the MAXED algorithm employs an iterative dual-annealing process using a detector response and an initial guess spectrum in conjunction with the DRM to find a spectrum that most closely gives the detector response [14]. Ideally, the guess spectrum starts the iterations in the phase space closest to the true spectrum. The results from this algorithm rely heavily on the initial guess and the solution cannot be proven to be the true spectrum.

3.2. Neural Network Approach

In addition to using MAXED to unfold the spectrum from the PNS detector response, a neural network approach was also explored. It has been proven that for any function, there exists a feed-forward deep neural network that can accurately represent that function [15,16]. In the last two decades, neural networks have taken immense strides in capability and reliability [17], spurred on by advances in computational power as well as new techniques for selecting and training hyperparameters. In 2012, a group of scientists made a network that superseded the performance of humans at pattern recognition[18]. In the years since, the capabilities of artificial intelligence have skyrocketed. This can be seen through networks like DALL-E, which can generate realistic images from a text prompt [19], and the recent release of GPT4, the most advanced multimodal model [20].

Developing and coding machine learning architecture has been streamlined through platforms and libraries such as TensorFlow [21]. These platforms provide a mechanism to be able to reliably code a machine learning model with built-in functions for widely accepted and used hyperparameters [21]. Now that complex

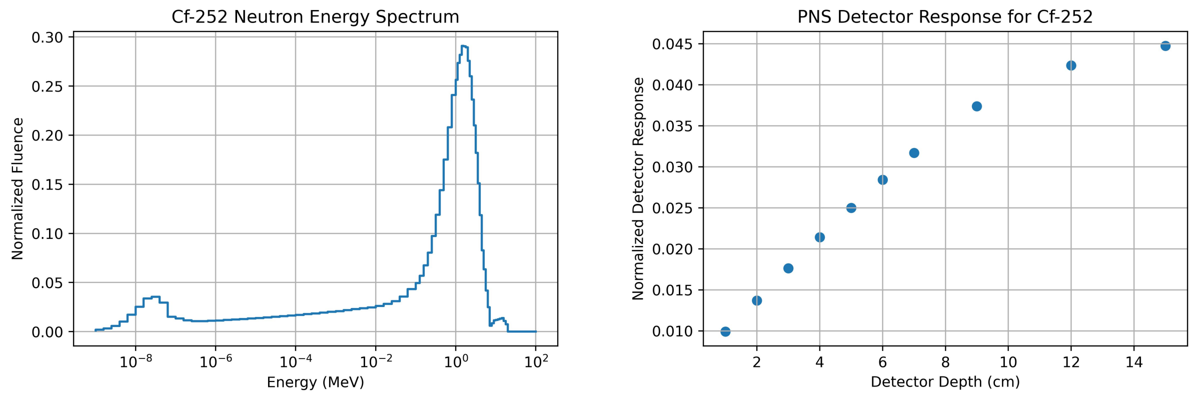

(a) Cf-252 Energy Spectrum **(b) Detector response calculated from DRM**

Figure 4: Cf-252 energy spectrum and DR calculated using this spectrum and the DRM

architectures can be developed easily, the biggest obstacle to obtaining an accurate model is having enough data to train it. Training data consists of an input with the associated output, and for this research, the input is a detector response while the output is a neutron energy spectrum. The IAEA provides a compendium of 251 neutron spectra in various environments [7]. Using the DRM for the PNS, each spectrum can be use to determine the corresponding detector response. This provides a data set containing 251 inputs and outputs to train a neural network. An example neutron energy spectrum with the associated detector response is shown in Figs. 4a and 4b.

3.2.1. Neural Network Structure

Neural networks have a variety of different architectures and methods for performing generally the same task: take input data and compute the answer [22]. For this research, a deep feed-forward neural network structure was chosen. An example network with this kind of structure is shown in Fig. 5. Each circle represents a neuron while each line represents the weight value with which each neuron is connected by an activation function to the next neuron. In this research, the left-most layer consists of 10 neurons, representing each value of the depth-averaged detector response. The right-most layer consists of 84 neurons, representing the energy spectrum, binned into 84 energy bins. The middle layers, called the hidden layers, are described below.

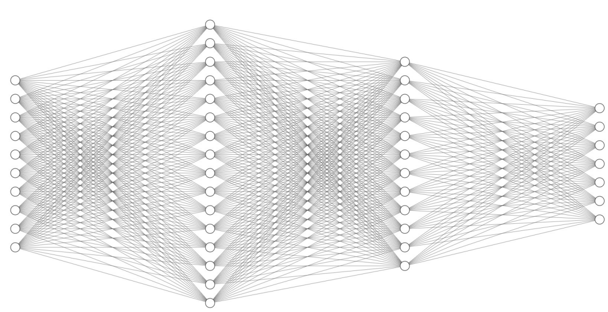

Figure 5: Visualization of an example neural network

Generally, the hidden layers of feed-forward networks have a descending number of neurons when visualized like Fig. 5. Although multiple optimization techniques, like Bayesian Optimization [23], exist to

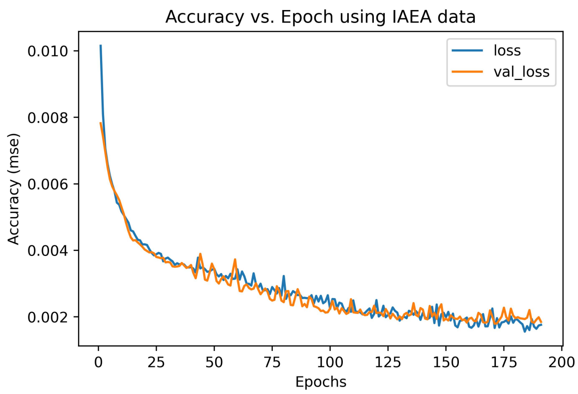

(a) **Training performance of NN**

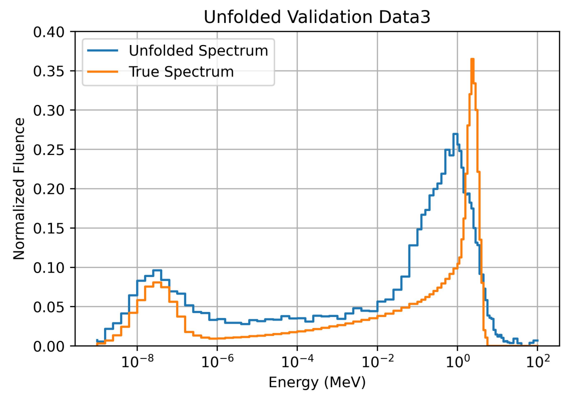

(b) **Example validation fit**

Figure 6: The training performance of the NN (6a) and an example fit from the validation set (6b)

fine-tune the hyperparameters to develop the best model, this research focused on defining hyperparameters that shows the viability of using neural networks for unfolding the PNS detector response. Several parameters need to be chosen before training a neural network. Namely, these parameters are the number of hidden layers, the number of neurons per hidden layer, and the activation function for each layer. To prevent overfitting, dropout layers may be added in between each hidden layer [22]. Additionally, early stopping criteria can be used to stop the training process before the network is overfit to the training data. Finally, all of the weights and biases are initially set pseudo-randomly and are adjusted during the training process.

3.2.2. Neural Network Training

The exact structure of this network is as follows:

- Input Layer: 10 neurons
- Hidden Layer 1: 512 neurons, activation=ReLU, dropout=0.3
- Hidden Layer 2: 256 neurons, activation=ReLU, dropout=0.3
- Hidden Layer 3: 128 neurons, activation=ReLU, dropout=0.3
- Output Layer: 84 neurons

As mentioned above, the number of neurons in each hidden layer decreases in the direction of the output layer. The activation function chosen was the ReLU function, shown in Eq. (2)

$$f(x) = \max(0, x). \tag{2}$$

Additionally, during training 30% of the neurons would be randomly dropped out per epoch, helping to prevent overfitting.

To train the network, the data set developed from the IAEA spectra was used. The data was split into 70% training and 30% validation. Following the data split, the training input and validation input were scaled to zero mean and unit variance separately to avoid cross-contamination between training and validation data. To train the network, the model was compiled using the mean-squared-error loss function with the Adam optimizer. Early stopping was also used to prevent overfitting.

4. RESULTS

Both unfolding algorithms were tested using real-world detector response data from the PNS in the presence of four different neutron sources: Cf-252, AmBe, the Godiva reactor, and the National Ignition Facility (NIF) [24].

4.1. MAXED Results

As mentioned in Section 3.1, the MAXED algorithm requires the detector response as well as the DRM and a guess spectrum. For a guess that is very close to the true spectrum, the algorithm can fairly closely match the true spectrum. These results are shown in Figs. 7a, 7c, and 7e. As the guess spectrum differs more from the true spectrum, the results of MAXED become less reliable. See Figs. 7b, 7d, and 7f for examples.

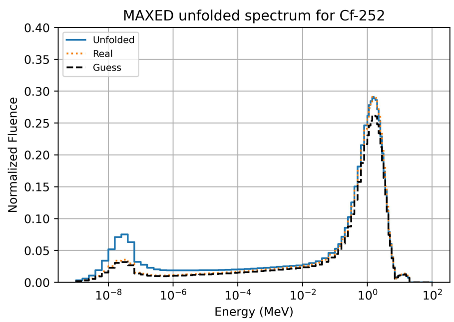

(a) Guess spectrum = 0.9*true Cf-252 spectrum

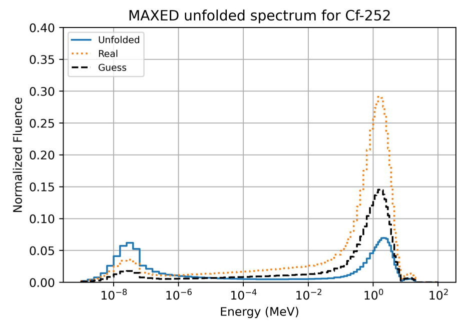

(b) Guess spectrum = 0.5*true Cf-252 spectrum

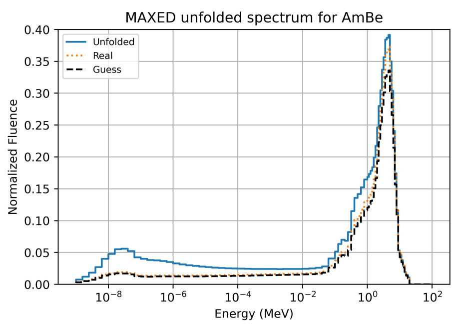

(c) Guess spectrum = 0.9*true AmBe spectrum

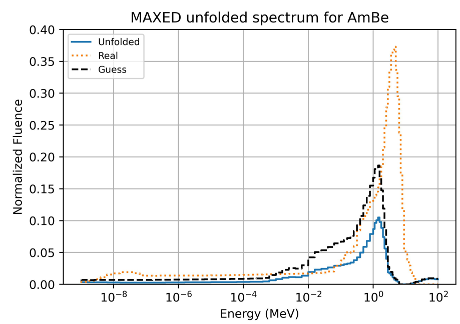

(d) Guess spectrum = 0.5*true AmBe spectrum

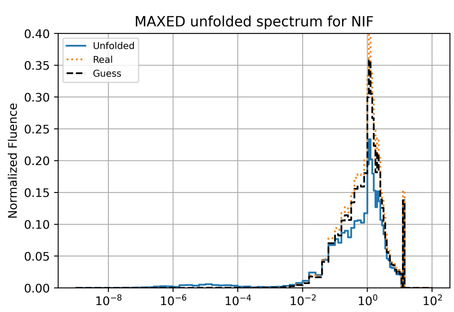

(e) Guess spectrum = 0.9*true NIF spectrum

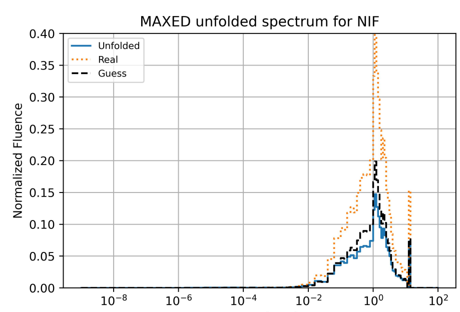

(f) Guess spectrum = 0.5*true NIF spectrum

Figure 7: Several unfolded spectra using the MAXED algorithm

4.2. Neural Network Results

In comparison to the MAXED algorithm, the neural network developed in this research requires only the detector response as an input. The results for the same neutron sources are shown in Figs. 8a to 8c. Additionally, a detector response from the Godiva reactor at White Sands Missile Range was input to the network and the unfolded spectrum is shown in Fig. 8d. Due to the limited number of training data, the results of the neural network are less accurate compared to MAXED results.

It can be noted that the unfolded spectra in Fig. 8 have similar features. This is largely due to the limited nature of the IAEA data set used to train the network. About 50% of this data set are spectra from a fission or moderated fission source and can cause a bias in the network. A larger data set, such as those proposed by [25] or [26], and an optimized neural network structure will be tested for better results.

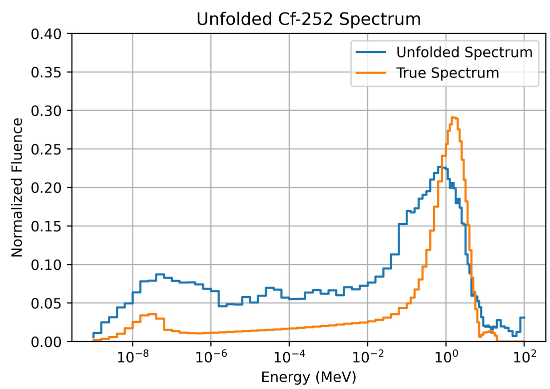

(a) Neural network unfolded Cf-252 Spectrum

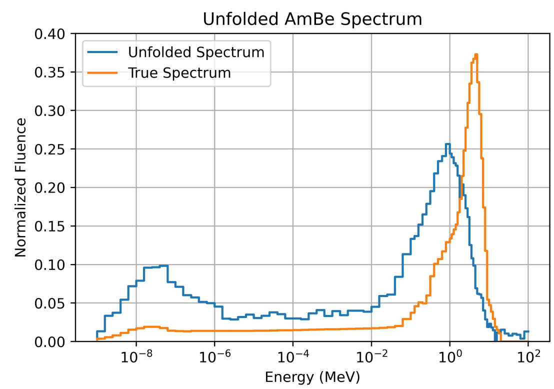

(b) Neural network unfolded AmBe Spectrum

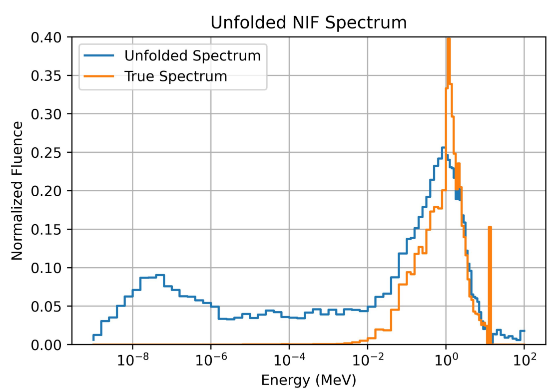

(c) Neural network unfolded NIF spectrum

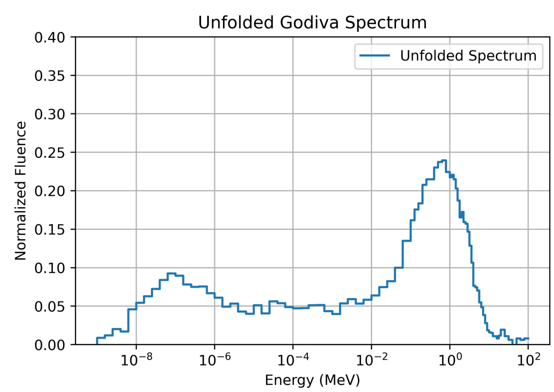

(d) NN unfolded Godiva spectrum

Figure 8: Several unfolded spectra using the neural network

5. CONCLUSION

This preliminary work has shown that the PNS has the capability to provide the information needed to unfold a neutron spectrum. Two techniques were used to unfold the spectrum: the maximum entropy deconvolution method, MAXED, and a neural network approach. At this point, MAXED was able to attain a more accurate result, given a guess spectrum that is close to the true spectrum. In future work, various avenues are available to create a better neural network for unfolding. These avenues include using different techniques to generate artificial neutron spectra to increase the training data set, using Bayesian optimization algorithms to choose better hyperparameters, and using other neural network architectures, such as convolutional neural networks. An encoder-decoder network structure developed for biomedical image segmentation, named UnetUnfold, has had promising results for unfolding neutron spectra [27]. This type of network as well as other more comprehensive networks will be explored in future work.

ACKNOWLEDGEMENTS

The views expressed in this article are those of the author and do not reflect the official policy or position of the United States Air Force, Department of Defense, or the U.S. Government.

Z. Condon thanks the Air Force Institute of Technology for providing financial support.

REFERENCES

[1] DOE-STD-1098. “DOE Standard: Radiological Control.” (2017).

[2] *Preparedness and Response for a Nuclear or Radiological Emergency. GSR Part 7*. General Safety Requirements. International Atomic Agency (2015).

[3] F. D. Brooks and H. Klein. “Neutron spectrometry - Historical review and present status.” *Nuclear Instruments and Methods in Physics Research, Section A: Accelerators, Spectrometers, Detectors and Associated Equipment*, **volume 476** (2002).

[4] G. F. Knoll. *Radiation detection and measurement*. John Wiley (2020).

[5] T. E. Johnson and H. Cember. *Introduction to health physics*. McGraw-Hill Education (2017).

[6] J. Kopecky, J.-C. Sublet, J. Simpson, R. Forrest, and D. Nierop. “Atlas of neutron capture cross sections.” Technical report, International Atomic Energy Agency (1997).

[7] R. V. Griffith, J. Pálfalvi, and U. Madhvanath. “Compendium of neutron spectra and detector responses for radiation protection purposes.” (1990).

[8] M. Wu, T. Guung, C. Pei, T. Yang, W. Hwang, and D. Thomas. “Absolute neutron fluence measurements between 0.5 and 3MEV and their intercomparisons.” *Nuclear Instruments and Methods in Physics Research Section A: Accelerators, Spectrometers, Detectors and Associated Equipment*, **volume 422**(1-3), p. 79–83 (1999).

[9] N. Colonna and G. Tagliente. “Response of liquid scintillator detectors to neutrons of ENlt;1 MeV.” *Nuclear Instruments and Methods in Physics Research Section A: Accelerators, Spectrometers, Detectors and Associated Equipment*, **volume 416**(1), p. 109–114 (1998).

[10] R. L. Bramblett, R. I. Ewing, and T. Bonner. “A new type of neutron spectrometer.” *Nuclear Instruments and Methods*, **volume 9**(1), p. 1–12 (1960).

[11] J. Gómez-Ros, R. Bedogni, M. Moraleda, A. Delgado, A. Romero, and A. Esposito. “A multi-detector neutron spectrometer with nearly isotropic response for environmental and workplace monitoring.” *Nuclear Instruments and Methods in Physics Research Section A: Accelerators, Spectrometers, Detectors and Associated Equipment*, **volume 613**(1), pp. 127–133 (2010).

[12] R. Bedogni, A. Calamida, T. Napolitano, C. Cantone, A. Fontanilla, A. C. Campoy, G. Abbatini, A. Pietropaolo, V. Monti, E. Mafucci, et al. “The NCT-WES directional neutron spectrometer: validation of the response with monoenergetic neutron fields.” *The European Physical Journal Plus*, **volume 138**(3), p. 270 (2023).

[13] J. A. Kulesza, T. R. Adams, J. C. Armstrong, S. R. Bolding, F. B. Brown, J. S. Bull, T. P. Burke, A. R. Clark, R. A. Forster, III, J. F. Giron, T. S. Grieve, C. J. Josey, R. L. Martz, G. W. McKinney, E. J. Pearson, M. E. Rising, C. J. Solomon, Jr., S. Swaminarayan, T. J. Trahan, S. C. Wilson, and A. J. Zukaitis. “MCNP® Code Version 6.3.0 Theory & User Manual.” Technical Report LA-UR-22-30006, Rev. 1, Los Alamos National Laboratory, Los Alamos, NM, USA (2022). URL https://www.osti.gov/biblio/1889957.

[14] M. Reginatto and P. Goldhagen. "MAXED, a computer code for the deconvolution of multisphere neutron spectrometer data using the maximum entropy method." Technical report, Dept. of Energy (1998).

[15] G. Cybenko. "Approximation by superpositions of a sigmoidal function." *Mathematics of control, signals and systems*, **volume 2**(4), pp. 303–314 (1989).

[16] M. A. Nielsen. *Neural networks and deep learning*, volume 25. Determination press San Francisco, CA, USA (2015).

[17] G. E. Hinton, S. Osindero, and Y.-W. Teh. "A fast learning algorithm for deep belief nets." *Neural computation*, **volume 18**(7), pp. 1527–1554 (2006).

[18] D. Ciregan, U. Meier, and J. Schmidhuber. "Multi-column deep neural networks for image classification." In *2012 IEEE conference on computer vision and pattern recognition*, pp. 3642–3649. IEEE (2012).

[19] K. Johnson. "OpenAI debuts dall-e for generating images from text." (2021). URL https://venturebeat.com/business/openai-debuts-dall-e-for-generating-images-from-text/.

[20] OpenAI. "GPT-4 Technical Report." (2023).

[21] "Tensorflow." URL https://www.tensorflow.org/.

[22] K. P. Murphy. *Probabilistic Machine Learning: An introduction*. MIT Press (2022).

[23] J. Snoek, O. Rippel, K. Swersky, R. Kiros, N. Satish, N. Sundaram, M. Patwary, M. Prabhat, and R. Adams. "Scalable bayesian optimization using deep neural networks." In *International conference on machine learning*, pp. 2171–2180. PMLR (2015).

[24] N. Quartemont, J. Bevins, N. Gharibyan, and K. Moody. "Spectral Shaping of NIF Characteristic 14 MeV Neutron Output." *LLNL-JRNL-813465* (2020).

[25] J. McGreivy, J. J. Manfredi, and D. Siefman. "Data Augmentation for Neutron Spectrum Unfolding with Neural Networks." *Journal of Nuclear Engineering*, **volume 4**(1), pp. 77–95 (2023).

[26] M. Bouhadida, M. Brovenchenko, T. Vinchon, W. Monange, and F. Trompier. "Neutron spectra reconstruction based on an artificial neural network trained with a large built dataset." In *ICRS 14/RPSD 2022 (14th International Conference on Radiation Shielding and 21st Topical Meeting of the Radiation Protection and Shielding Division)* (2022).

[27] M. Bouhadida, A. Mazzi, M. Brovchenko, T. Vinchon, M. Z. Alaya, W. Monange, and F. Trompier. "Neutron spectrum unfolding using two architectures of convolutional neural networks." *Nuclear Engineering and Technology* (2023).